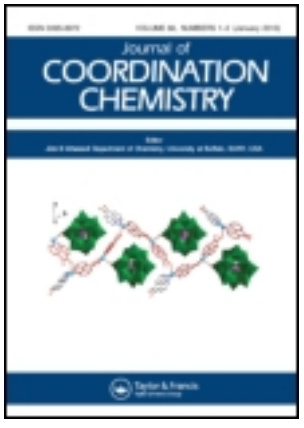

Journal of Coordination Chemistry
Publication details, including instructions for authors and subscription information:
http://www.tandfonline.com/loi/gcoo20

Coordination polymers constructed from an asymmetric dicarboxylate and N-donors: preparation, characterization, and properties

Xiao-Li Chen[a], Ya-Li Qiao[a], Lou-Jun Gao[a] & Mei-Li Zhang[a]
[a] Department of Chemistry and Chemical Engineering, Shaanxi Key Laboratory of Chemical Reaction Engineering, Yanan University, Yan'an, P.R. China
Accepted author version posted online: 07 Oct 2013.Published online: 15 Nov 2013.

To cite this article: Xiao-Li Chen, Ya-Li Qiao, Lou-Jun Gao & Mei-Li Zhang (2013) Coordination polymers constructed from an asymmetric dicarboxylate and N-donors: preparation, characterization, and properties, Journal of Coordination Chemistry, 66:21, 3749-3759, DOI: 10.1080/00958972.2013.852186

To link to this article: http://dx.doi.org/10.1080/00958972.2013.852186

Journal of Coordination Chemistry, 2013
Vol. 66, No. 21, 3749–3759, http://dx.doi.org/10.1080/00958972.2013.852186

Coordination polymers constructed from an asymmetric dicarboxylate and N-donors: preparation, characterization, and properties

XIAO-LI CHEN*, YA-LI QIAO, LOU-JUN GAO and MEI-LI ZHANG

Department of Chemistry and Chemical Engineering, Shaanxi Key Laboratory of Chemical Reaction Engineering, Yanan University, Yan'an, P.R. China

(*Received 26 December 2012; accepted 21 August 2013*)

Two new coordination polymers with an asymmetric dicarboxylate and 4,4′-bipyridine ligand, {[Co(bpy)(H_2O)$_4$]·(cpa)·0.5H_2O}$_n$ (**1**) and {[Ag(cpa)(bpy)][Ag(bpy)]·4H_2O}$_n$ (**2**) (H_2cpa = 4-(2-carboxyethyl)benzoic acid, bpy = 4,4′-bipyridine), have been hydrothermally synthesized and characterized by elemental analysis, FT-IR spectroscopy, and single-crystal X-ray diffraction. Compound **1** displays a chain with guest molecule $(cpa)^{2-}$ ions existing in the structure. Compound **2** contains two independent units, $[Ag(cpa)(bpy)]^-$ (**A**) and $[Ag(bpy)]^+$ (**B**), which form a 1-D + 1-D structure. **A** shows a 1-D chain structure bearing hooks formed by the carboxylates and organized into a tubular structure by hydrogen-bonding interactions. **B** has linear chains formed from Ag^+ and bpy. The **A** and **B** chains co-crystallize with waters of crystallization to provide two linear $[Ag(bpy)]^+$ chains embedded in the tubular structure formed by **A** via $\pi...\pi$ stacking contacts. In **1** and **2**, hydrogen-bonding and $\pi...\pi$ stacking interactions connect the discrete 1-D chains into 3-D supramolecular structures. The fluorescent properties, TG analysis, and X-ray powder diffraction patterns for **1** and **2** were also measured.

Keywords: Coordination polymer; Hydrothermal synthesis; Crystal structure; Fluorescence

1. Introduction

The crystal engineering of metal–organic frameworks attracts intense attention because controlling the molecular organization in the solid state can lead to materials with new structures and promising properties [1–8]. To build these molecular architectures with interesting compositions and topologies, judicious selection of appropriate polydentate organic ligands and metal ions is key [9–13]. The former is mainly concerned with assembly of molecular building blocks into well-defined crystalline structures via non-covalent bonds, while the latter relies on stronger coordinate bonds to form extended networks by using polydentate ligands [14]. Polycarboxylates are often employed as bridging ligands to construct metal–organic coordination frameworks owing to their versatile coordination and ability to act as H-bond acceptors and donors in assembling supramolecular structures [15–21]. Investigation of unsymmetrical dicarboxylates are fewer than symmetrical dicarboxylates.

*Corresponding author. Emails: chenxiaoli003@163.com, yadxhgxy@163.com

The ligand 4-(2-carboxyethyl)benzoic acid (H_2cpa) is an interesting building block, mainly due to the possibility of different coordination sites, as well as its rigidity and flexibility [22, 23]. In these examples, the geometric disposition of the carboxylate arms and the nature of the neutral tethering ligand play a dominant role in the final structure. However, few compounds based on H_2cpa have been documented [22, 23]. Combination of metal ions with neutral N-donor ligands can generate interesting structures, which cannot be obtained through only one type of ligand. Structural elaboration and topological variance in these complexes can be enhanced by incorporation of neutral ligands such as 4,4′-bipyridine (bpy), 1,2-bis(4-pyridyl)ethylene (dpee), 1,2-bis(4-pyridyl)ethane (dpe), or 1,10-phenanthroline (phen) via adjustment of the carboxylate bridge [24–26]. A number of cobalt(II) and silver(I) coordination polymers have been constructed from polycarboxylates such as phthalate [27], terephthalate [28], isophthalate [29], biphenyl-2,2′,4,4′-tetracarboxylic acid [30], 3,3′,4,4′-benzophenonetetracarboxylic [31], and pyrazine-2,3,5,6-tetracarboxylic acid [32], which provide both the charge balance and structural rigidity necessary for self-assembly. We have recently synthesized compounds with H_2cpa and bpy and have now isolated two new compounds, $\{[Co(bpy)(H_2O)_4]\cdot(cpa)\cdot 0.5H_2O\}_n$ (**1**) and $\{[Ag(cpa)(bpy)][Ag(bpy)]\cdot 4H_2O\}_n$ (**2**). A detailed structural analysis of **1** and **2** proved the significance of the hydrogen bonds and $\pi...\pi$ stacking interactions in extending the structures into 3-D supramolecular frameworks. **2** is a Ag(I) coordination polymer with two types of ionic 1-D chains. The anion shows a 1-D chain structure bearing hooks formed from carboxylates and organized into a tubular structure by hydrogen-bonding interactions. The cation is also a linear chain. Two linear cationic chains are embedded in the tubular structure by $\pi...\pi$ stacking interactions. The structural differences demonstrate that metal ions have significant effects on formation and structures of the final metal–organic coordination polymers. Herein, the syntheses, structures, thermal stability, and photoluminescence of **1** and **2** are described.

2. Experimental

2.1. *Materials and physical measurements*

All chemicals and reagents were used as received from commercial sources without purification. All reactions were carried out under hydrothermal conditions. Elemental analyzes (C, H, and N) were determined with an Elementar Vario EL III elemental analyzer. IR spectra were recorded as KBr pellets on a Bruker EQUINOX55 spectrophotometer from 4000 to 400 cm^{-1}. Fluorescence spectra were obtained on a Hitachi F-4500 fluorescence spectrophotometer at room temperature. Thermogravimetric analyzes (TGA) were performed in a nitrogen atmosphere with a heating rate of 10 °C min^{-1} with a NETZSCH STA 449C thermogravimetric analyzer. X-ray powder diffraction patterns were recorded with a Pigaku D/Max 3III diffractometer. The powder X-ray diffraction (PXRD) of a dehydrated sample of **2** was measured after **2** was dried in a vacuum drying box for two hours at 200 °C.

2.2. *Synthesis of $\{[Co(bpy)(H_2O)_4]\cdot(cpa)\cdot 0.5H_2O\}_n$ (1)*

A mixture of $Co(NO_3)_2\cdot 6H_2O$ (0.0291 g, 0.1 mM), H_2cpa (0.0194 g, 0.1 mM), bpy (0.0156 g, 0.1 mM), and NaOH (0.008 g, 0.2 mM) in water (10 mL) was stirred for 30 min

in air, then sealed in a 25-mL Teflon-lined stainless steel container, which was heated to 160 °C for 96 h. After cooling to room temperature at a rate of 5 °C h^{-1}, yellow block crystals were obtained. Yield: 0.0308 g (63% based on H_2cpa). Anal. Calcd for $C_{20}H_{25}CoN_2O_{8.5}$ (%): C, 49.19; H, 5.16; N, 5.74. Found: C, 49.22; H, 5.14; N, 5.78. IR (KBr cm^{-1}): 3295m, 1544s, 1513m, 1430m, 1392vs, 1290s, 1180w, 1108w, 966w, 856s, 763s, 728s, 663w, 633w.

2.3. *Synthesis of {[Ag(cpa)(bpy)][Ag(bpy)]·4H$_2$O}$_n$ (2)*

A procedure identical with that for **1** was followed to prepare **2**, except that Co $(NO_3)_2·6H_2O$ was changed to $AgNO_3$ (0.0169 g, 0.1 mM). Colorless crystals were obtained. Yield: 0.0460 g (58% based on Ag). Anal. Calcd for $C_{30}H_{32}Ag_2N_4O_8$ (%): C, 45.48; H, 4.07; N, 7.07. Found: C, 45.51; H, 4.02; N, 7.05. IR (KBr cm^{-1}): 3449s, 1580s, 1553s, 1407m, 1380vs, 1210w, 1148w, 1060w, 878w, 814s, 780w, 735w, 664w.

2.4. *X-ray crystallography*

Intensity data were collected on a Bruker Smart APEX II CCD diffractometer with graphite-monochromated Mo Kα radiation (λ = 0.71073 Å) at room temperature. Empirical absorption corrections were applied using SADABS. The structures were solved by direct methods and refined by full-matrix least-squares based on F^2 using SHELXTL-97 [33]. All non-hydrogen atoms were refined anisotropically, and hydrogens of organic ligands were generated geometrically. Hydrogens of coordinated water were located in the difference Fourier map and refined with restrained O–H bond lengths [0.85(2) Å] and refined fixed isotropic displacement parameters $U_{iso}(H) = 1.2U_{eq}(O)$. Crystal data and structural refinement parameters for **1** and **2** are summarized in table 1. Selected bond distances and angles are listed in table 2. Hydrogen-bond distances and angles are listed in table 3.

Table 1. Crystal data and structural refinement parameters for **1** and **2**.

Compound	**1**	**2**
Empirical formula	$C_{40}H_{48}Co_2N_4O_{17}$	$C_{30}H_{30}Ag_2N_4O_7$
Formula weight	974.68	774.32
Crystal system	Monoclinic	Monoclinic
Space group	*P2(1)/c*	*C2/c*
a/Å	12.2121(13)	13.9833(19)
b/Å	13.3343(14)	17.9852(19)
c/Å	14.2535(15)	22.788(3)
α/°	90	90
β/°	113.8290(10)	97.846(3)
γ/°	90	90
V/Å^3	2123.2(4)	5677.3(12)
Z	2	8
ρ_{Calcd}/g cm^{-3}	1.531	1.812
F (000)	1020	3104
Reflections collected	10,380	14,162
S on F^2	1.060	1.058
R_1, wR_2[a] [$I > 2\sigma(I)$]	0.0317, 0.0787	0.0614, 0.1111
R_1, wR_2[a] (all data)	0.0368, 0.0821	0.0924, 0.1246

[a]$R_1 = \Sigma||F_o| - |F_c||/\Sigma|F_o|$, $wR_2 = [\Sigma w(F_o^2 - F_c^2)^2/\Sigma w(F_o^2)^2]^{1/2}$.

Table 2. Selected bond distances and angles for **1** and **2**.

Compound **1**			
Co(1)–O(2)	2.0813(17)	Co(1)–O(1)	2.0887(18)
Co(1)–O(3)	2.0953(17)	Co(1)–O(4)	2.0976(16)
Co(1)–N(1)	2.1611(18)	Co(1)–N(2)#1	2.1616(18)
O(2)–Co(1)–O(1)	90.61(8)	O(2)–Co(1)–O(3)	96.68(8)
O(1)–Co(1)–O(3)	172.67(7)	O(2)–Co(1)–O(4)	175.14(7)
O(1)–Co(1)–O(4)	85.09(7)	O(3)–Co(1)–O(4)	87.59(7)
O(2)–Co(1)–N(1)	88.30(7)	O(1)–Co(1)–N(1)	91.93(7)
O(3)–Co(1)–N(1)	87.62(7)	O(4)–Co(1)–N(1)	89.57(7)
O(2)–Co(1)–N(2)#1	87.49(7)	O(1)–Co(1)–N(2)#1	90.86(7)
O(3)–Co(1)–N(2)#1	90.15(7)	O(4)–Co(1)–N(2)#1	94.84(7)
N(1)–Co(1)–N(2)#1	174.97(7)		
Compound **2**			
Ag(1)–N(1)	2.199(5)	Ag(1)–N(2) #1	2.217(5)
Ag(1)–O(1)	2.386(5)	Ag(2)–N(4)#2	2.151(5)
Ag(2)–N(3)	2.155(5)		
N(1)–Ag(1)–O(1)	102.92(17)	N(1)–Ag(1)–N(2)#1	157.49(19)
N(2)#1–Ag(1)–O(1)	96.11(17)	N(4)#2–Ag(2)–N(3)	175.6(2)

Notes: Symmetry codes for **1**: #1 $x + 1, -y + 1/2, z + 1/2$; #2 $x - 1, -y + 1/2, z - 1/2$; #3 $-x + 2, -y + 2, -z$. For **2**: #1 $x, -y, z - 1/2$; #2 $x, -y + 2, z + 1/2$.

3. Results and discussion

3.1. *Description of crystal structure*

3.1.1 $\{[Co(bpy)(H_2O)_4]\cdot(cpa)\cdot 0.5H_2O\}_n$ (1). X-ray single-crystal diffraction analysis revealed that **1** is a salt consisting of a one-dimensional linear chain formed from Co^{2+} and with uncoordinated $(cpa)^{2-}$ balancing the overall charge and attached to the cation via hydrogen bonds with coordinated water. As shown in figure 1(a), each Co(II) is octahedrally coordinated by two pyridyl N [Co(1)–N(1) = 2.1610(18), Co(1)–N(2A) = 2.1616(18) Å] from two different 4,4′-bpy ligands and four O of water. The Co–O distances, 2.0815(17)-2.0976 (16) Å, are comparable to those in $\{[Co(bpdc)(H_2O)_3]\cdot H_2O\}_n$ (bpdc = 2,2′-bipyridyl-3,3′-dicarboxylic acid) [34]. Each bpy bridges two Co^{2+} to form a linear chain structure with Co…Co distance of 11.401(2) Å (figure 1(b)). The two pyridyl rings of 4,4′-bpy are not coplanar, presenting a dihedral angle of 26.82°, which is smaller than the corresponding value of 33.8° in $[Co(bpy)_2(H_2O)_4]$ ASCl·$3H_2O$ (AS = amino-salicylate anion), although the bond distances in **1** and $[Co(bpy)_2(H_2O)_4]$ ASCl·$3H_2O$ are similar [35]. The overall structure is similar to $[Co_2(bpy)_6]\cdot(btca)\cdot Cl\cdot 11H_2O$ (btca = benzene-1,3,5-tricarboxylate, bpy = 2,2′-bipyridine) [36], in which Co^{2+} only coordinates two 2,2′-bpy ligands to generate the cationic unit $[Co_2(bpy)_6]^{2+}$, while one $btca^{3-}$, a chloride, and 11 uncoordinated waters are contained in the structure. Hydrogen-bonding interactions play an important role in stabilizing **1**. A significant feature is that adjacent linear chains interact with each other to generate a 3-D supramolecular framework via hydrogen-bonding interaction between the carboxylates O5, O6, O7, and O8 from uncoordinated $(cpa)^{2-}$ and O1, O2, O3, and O4 from coordinated water (figure 1(c)).

3.1.2 $\{[Ag(cpa)(bpy)][Ag(bpy)]\cdot 4H_2O\}_n$ (2). When Co^{2+} is replaced by a Ag^+ with larger radius, a different structure was formed under similar reaction conditions. **2** is a salt comprised of two distinct and crystallographically independent units, $[Ag(cpa)(bpy)]^-$ (**A**) and $[Ag(bpy)]^+$ (**B**), which form an integrated 1-D + 1-D structure via $\pi...\pi$ stacking

Table 3. Hydrogen bond distances (Å) and angles (°) for **1** and **2**.

D–H...A	*d*(*D–H*)	*D*(*H...A*)	*d*(*D...A*)	<(*DHA*)
Compound **1**				
O1^{i}–H1A...O6^{iii}	0.82(2)	1.92(2)	2.725(2)	167(3)
O1–H1B...O9^{iii}	0.79(3)	2.01(4)	2.685(5)	143(3)
O1–H1B...O7^{iv}	0.79(3)	2.47(2)	3.140(4)	143(3)
O2^{i}–H2A...O5^{ii}	0.82(3)	1.91(3)	2.691(3)	159(3)
O2^{i} –H2B...O8^{iv}	0.84(3)	1.93(3)	2.763(3)	170(3)
O3–H3A...O6^{ii}	0.85(3)	1.74(3)	2.594(3)	178(3)
O3–H3B...O8	0.83(2)	2.06(2)	2.847(3)	158(3)
O4–H4A...O8	0.82(2)	1.93(2)	2.735(2)	168(3)
O4–H4B...O5^{iii}	0.84(2)	1.80(2)	2.633(2)	171(2)
Compound **2**				
O5–H5A...O6^{v}	0.83(5)	1.95(5)	2.778(7)	174 (7)
O6–H6A...O1^{ii}	0.83(6)	1.91(6)	2.734(8)	174(6)
O6–H6B...O3^{iii}	0.85(2)	1.86(3)	2.696(6)	167(8)
O7–H7A...O2^{iv}	0.85(7)	2.00(6)	2.732(6)	145(9)
O8–H8A...O4^{i}	0.85(6)	2.05(6)	2.903(9)	172(9)
O8–H8B...O4^{vi}	0.84(7)	2.03(7)	2.836(9)	160(8)

Notes: Symmetry code for **1**: (i) *x*, –*y* + 1/2, *z* + 1/2; (ii) *x* + 1, –*y* + 1/2, *z* + 1/2; (iii) *x*, –*y* + 3/2, *z* + 1/2; (iv) *x*, –0.5 – *y*, 0.5 + *z*. For **2**: (i) *x*, –*y*, –0.5 + *z*; (v) 1.5 + *x*, 0.5 + *y*, 1 + *z*; (ii) 0.5 + *x*, 0.5 – *y*, –0.5 + *z*; (iii) 1 + *x*, *y*, 1 + *z*; (iv) 1.5 + *x*, 0.5 + *y*, *z*; (vi) 1 + *x*, *y*, *z*.

interactions. The asymmetric unit of **A** has one independent Ag^{+}, one bpy, and one $(cpa)^{2-}$. As shown in figure 2(a), Ag(1) is coordinated by N1 and N2A from two different bpy ligands and O1 of a monodentate carboxylate from $(cpa)^{2-}$. The Ag(1)–N(1) and Ag(1)–N(2A) bond lengths are 2.199(5) Å and 2.217(5) Å, respectively, whereas the Ag(1)–O(1) bond length is 2.386(5) Å, close to one in $[Ag(4,4'\text{-bipy})]_n$ $[Ag(HBTC)]_n$ [Ag–O = 2.348(3) Å] (H_3BTC = 1,2,4-benzenetricarboxylate acid) [37]. The N(1)-Ag(1)-N(2A) bond angle is 157.49(19)°. The pyridine rings of bpy are non-coplanar with a dihedral angle of 10.07°, and the Ag(1)…Ag(1) separation between each bpy is 11.483 Å. The coordination polyhedron of Ag^{+} can be described as T-shaped. Hence, the bpy ligands bridge Ag(1) centers to form a 1-D chain decorated with $(cpa)^{2-}$ as "hooks," with each "hook" alternating between each side of the chain (figure 2(b)). This is different from a reported Ag compound containing bpy and carboxylate ligands [38], in which the 1-D chains bear hooks formed with $(H_2cpop)^{-}$ [H_3cpop = 4-(4-carboxy-phenoxy)phthalic acid] only on the same side of the chain. Additionally, since H_3cpop is only partially deprotonated, each pair of $(H_2cpop)^{-}$ ligands from adjacent chains forms a head-to-tail 26-membered hydrogen-bonded ring. Because H_2cpa in **2** is completely deprotonated, each pair of $(cpa)^{2-}$ ligands from adjacent chains does not form a head-to-tail hydrogen-bonded ring.

Ag(2) is ligated by N1 and N2A from two different bpy ligands [Ag(2)–N(3) = 2.155(5), Ag(2)–N(4B) = 2.151(5) Å] to form a linear chain. These bond distances are shorter than those of the three-coordinate geometry in **A**, further indicating that the metal–ligand bond distance is closely related to its coordination geometry. The N(3)–Ag(2)–N(4B) bond angle is 175.6(2)°. The pyridine rings of bpy are non-coplanar with a dihedral angle of 9.38°, and the Ag2…Ag2 separation between each bpy is 11.394 Å. These values are smaller than the corresponding values in **A**. Two parallel linear chains of **B** are nearly completely overlapping, with Ag2…Ag2 separation of 3.395 Å, which is close to the van der Waals contact distance (3.40 Å), illustrating the existence of argentophilic interactions between Ag2 ions. The Ag…Ag distances in **B** are longer than those in $[Ag_8(btc)_2(2,2'\text{-bpy})_2]_n$ [btc = biphenyl-2,2′,4,4′-tetra-carboxylic acid), which displays two kinds of Ag–Ag interactions [30].

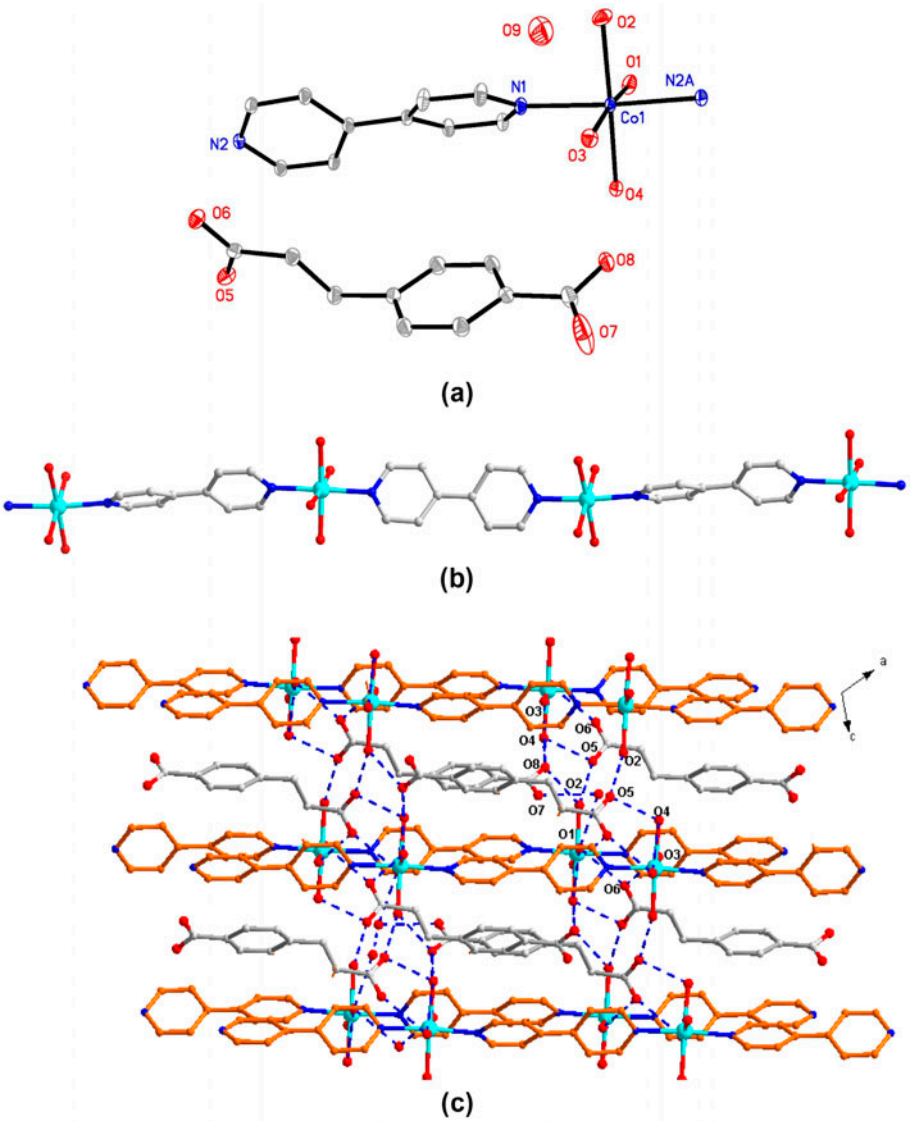

Figure 1. (a) The coordination environment of Co^{2+} in **1** with 30% probability displacement ellipsoids. (b) View of the linear chain. (c) The 3-D supramolecular structure based on O–H...O hydrogen bonds along the *b*-axis; all hydrogens are omitted for clarity.

One type is a strong Ag–Ag contact (Ag–Ag distances 2.8247(11) and 2.8051(12) Å), which is shorter than the Ag–Ag distance in metallic silver (2.88 Å). The other is a weaker Ag…Ag interaction (Ag–Ag distances 3.0073(11), 2.9268(11) Å, and 3.1606(12) Å), but whose distances are still below the van der Waals contact distance.

More interestingly, two **A** chains bearing hooks generate a 1-D tubular structure supported by hydrogen-bonding interactions with the waters of the structure. Two linear chains of **B** are embedded in the tubular structure by $\pi...\pi$ stacking interactions (figure 2(c)). So, the chains bearing hooks encircle the linear chains like a belt. The packing of **A** and **B** within the

tubular structure shows two kinds of $\pi...\pi$ stacking interactions, one between adjacent **B** chains and the other between the adjacent **A** and **B** chains, as shown in figure 2(d). The face-to-face distance between the pyridyl rings of adjacent bpy in the **B** chains is 3.363 Å (blue line). The face-to-face distance between the pyridyl rings of adjacent **A** and **B** chains is 3.399 Å (orange line). The face-to-face distance between the pyridyl rings of the **A** chains in adjacent tubular structures is 3.397 Å (green line). These $\pi...\pi$ stacking interactions are alternating and stabilize the stacked arrangement. The adjacent tubular structures further form a 3-D supramolecular micropore structure through O–H···O hydrogen bonds (figure 2(e)) and $\pi\ldots\pi$ stacking interactions (green line). The inner space of the 3-D network is filled with linear chains and lattice waters (figure 2(f)).

3.2. *Luminescence properties*

Emission spectra of H_2cpa and **2** in the solid state at room temperature are shown in figure 3. Unfortunately, **1** exhibited only a very weak emission. H_2cpa exhibited two

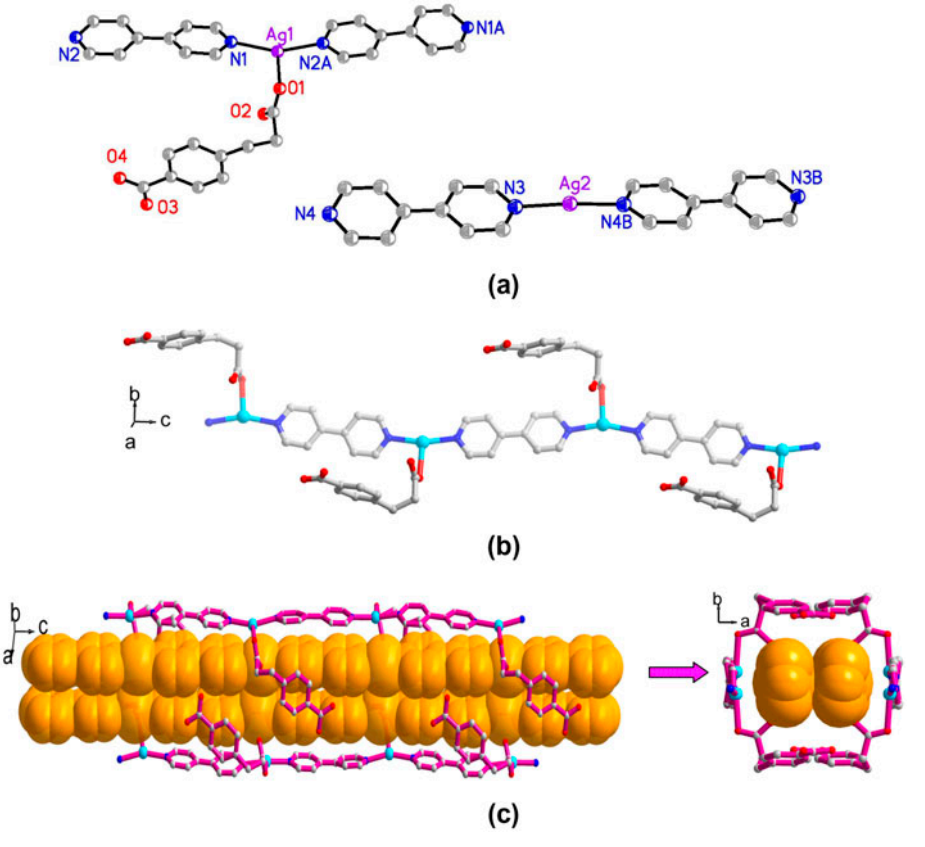

Figure 2. (a) Coordination environment of Ag^+ in **2** with 30% probability displacement ellipsoids. (b) View of the 1-D chain of **A**, illustrating the hooks formed from cpa^{2-}. (c) View of the 1-D tubular structure along the *c*-axis. (d) View of three kinds of $\pi...\pi$ stacking interactions (orange, green and blue) along the *c*-axis. (e) View of the 3-D networks through hydrogen bond (black), $\pi...\pi$ stacking (green) and Ag···Ag interactions (red) along the *c*-axis. (f) Perspective view of the 3-D supramolecular framework along the *c*-axis; all hydrogens are omitted for clarity (see http://dx.doi.org/10.1080/00958972.2013.852186 for color version).

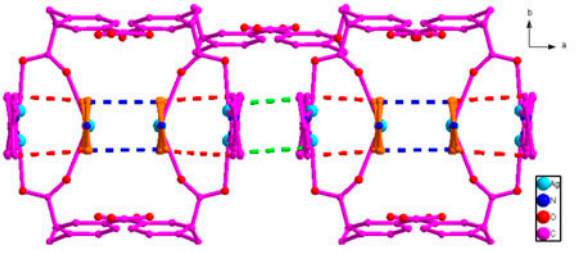

(d)

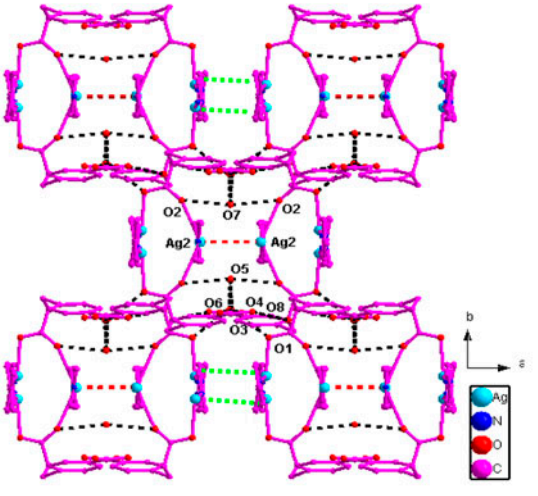

(e)

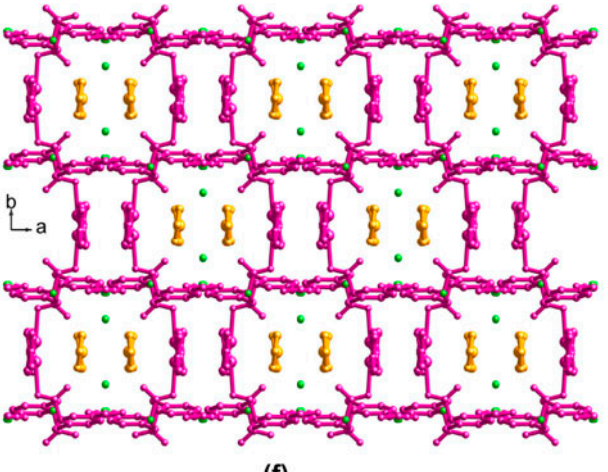

(f)

Figure 2. (*Continued*)

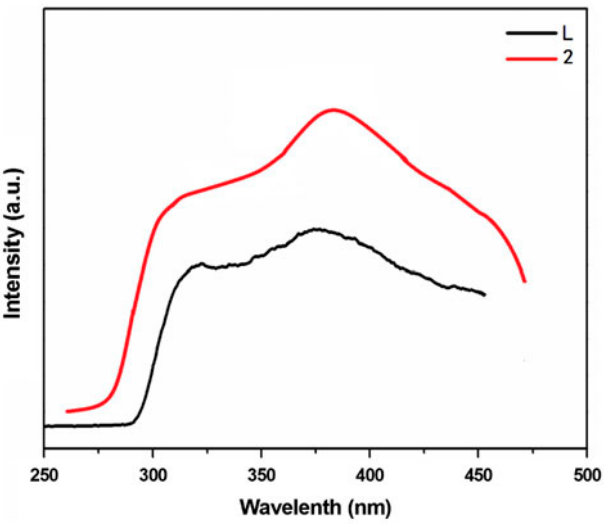

Figure 3. The emission spectra of H_2cpa and **2** in the solid state at room temperature.

emission bands at 323 nm and 377 nm upon excitation at 230 nm. Similar emissions at 325 and 382 nm were observed for **2** upon excitation at 240 nm. This suggests that the emission of **2** originates from the π–π^* electronic transition of ligand [39]. By comparing the emission spectra of **2** and H_2cpa, enhancement of luminescence in **2** may be attributed to its rigidity. This rigidity favors energy transfer and reduces the loss of energy through a radiationless pathway [40–43].

3.3. *PXRD pattern and thermal stability analysis*

To confirm the phase purity of the bulk materials, PXRD experiments were carried out on **1** and **2**. To document the good thermal stability of **2**, a PXRD of **2** was measured after heating at 200 °C under vacuum for 2 h. The experimental and computer-simulated PXRD patterns are shown in figure S1. Although minor differences can be seen in the positions, intensities, and widths of some peaks, the data demonstrate the phase homogeneity of the as-synthesized materials. The PXRD and TGA data (figure S2) of dehydrated **2** show that **2** retains its crystallinity even after removal of the waters of crystallization.

To measure the thermal stabilities of **1** and **2**, TGA measurements were carried out (figure S3). **1** lost lattice and coordinated waters below 195 °C. The weight loss of 16.2% is consistent with the calculated value (16.5%). A weight loss of 39.2% then occurs from 195 to 393 °C, corresponding to removal of cpa^{2-} (Calcd 39.4%). The third weight loss of 31.5% is observed from 393 to 445 °C and is consistent with that calculated (32.0%) for decomposition of bpy. The remaining weight of 16.8% corresponds to the final product CoO (Calcd 16.2%). **2** first lost lattice water below 180 °C; the weight loss of 6.89% is consistent with the calculated value (6.99%). **2** was then stable to 305 °C, followed by one-step weight loss from 305 to 565 °C, corresponding to decomposition of cpa^{2-} and bpy (found: 73.1%; Calcd 72.2%). The remaining weight of 27.4% is consistent with Ag_2O and is in agreement with the calculated value of 27.8%. The TGA results show that **2** has good thermal stability, likely because of its complex structure.

4. Conclusion

We synthesized and structurally characterized two new coordination polymers by appropriately combining different metal salts with H_2cpa in the presence of 4,4′-bpy. Compound **1** is a salt with a 1-D cationic linear chain and uncoordinated $(cpa)^{2-}$. Compound **2** contains two types of independent polymers, **A** and **B**, which form an integrated 1-D + 1-D structure. Comparison of **1** and **2** shows that different metal salts are a critical factor for formation and structure of the resulting compounds. The $\pi...\pi$ stacking interactions play a crucial role in stability of the structure of **2** and also influence the final supramolecular structure together with abundant hydrogen-bond interactions. **2** also displays luminescence resulting from the intraligand π–π* transition.

Supplementary material

Experimental and simulated PXRD patterns and TGA curves of **1**, **2**, and dehydrated **2**. Crystallographic data for the structural analyzes have been deposited with the Cambridge Crystallographic Data Center, CCDC Nos. 916609-916608 for **1** and **2**. Copies of the data can be obtained free of charge on application to CCDC, 12 Union Road, Cambridge CB2 1EZ, UK (Fax: internat.+44-1223-336-033; E-mail: deposit@ccdc.cam.ac.uk) Supplemental data for this article can be accessed http://dx.doi.org/10.1080/00958972.2013.852186.

Funding

This work was supported by the National Natural Science Foundation of China [grant number 21101133] and the Natural Scientific Research Foundation of Shaanxi Provincial Education Office of China [grant number 11JK0565], [grant number 11JK0567].

References

[1] S. Kitagawa, R. Kitaura, S. Noro. *Angew. Chem. Int. Ed.*, **43**, 2334 (2004).
[2] J.L.C. Rowsell, O.M. Yaghi. *Angew. Chem. Int. Ed.*, **44**, 4670 (2005).
[3] A.Y. Robin, K.M. Fromm. *Coord. Chem. Rev.*, **250**, 2127 (2006).
[4] Y.Y. Liu, J.F. Ma, J. Yang, J.C. Ma, Z.M. Su. *CrystEngComm.*, **10**, 894 (2008).
[5] M.R. Kishan, J. Tian, P.K. Thallapally, C.A. Fernandez, S.J. Dalgarno, J.E. Warren, B.P. McGrail, J.L. Atwood. *Chem. Commun.*, **46**, 538 (2010).
[6] M.D. Allendorf, C.A. Bauer, R.K. Bhakta, R.J.T. Houk. *Chem. Soc. Rev.*, **38**, 1330 (2009).
[7] J. Rocha, L.D. Carlos, F.A. Almeida Paz, D. Ananias. *Chem. Soc. Rev.*, **40**, 926 (2011).
[8] Y.Y. Karabach, M.F.C.G. Silva, M.N. Kopylovich, B. Gil-Hernández, J. Sanchiz, A.M. Kirillov, A.J.L. Pombeiro. *Inorg. Chem.*, **49**, 11096 (2010).
[9] C.P. Li, J. Chen, M. Du. *CrystEngComm.*, **12**, 4392 (2010).
[10] X.L. Wang, C. Qin, E.B. Wang, Y.G. Li, Z.M. Su, C.W. Hu, L. Xu. *Angew. Chem. Int. Ed.*, **43**, 5036 (2004).
[11] H.Y. An, E.B. Wang, D.R. Xiao, Y.G. Li, Z.M. Su, L. Xu. *Angew. Chem. Int. Ed.*, **45**, 904 (2006).
[12] Y.G. Huang, D.Q. Yuan, L. Pan, F.L. Jiang, M.Y. Wu, X.D. Zhang, W. Wei, Q. Gao, J.Y. Lee, J. Li, M.C. Hong. *Inorg. Chem.*, **46**, 9609 (2007).
[13] X.Z. Li, M. Li, Z. Li, J.Z. Hou, X.C. Huang, D. Li. *Angew. Chem. Int. Ed.*, **47**, 6371 (2008).
[14] D. Braga. *Acc. Chem. Res.*, **33**, 601 (2000).
[15] J. Kim, B. Chen, T.M. Reineke, H. Li, M. Eddaoudi, D.B. Moler, M. O'Keeffe, O.M. Yaghi. *J. Am. Chem. Soc.*, **123**, 8239 (2001).

[16] F. Guo, B.Y. Zhu, Y.L. Song, X.L. Zhang. *J. Coord. Chem.*, **63**, 1304 (2010).
[17] X.L. Wang, C. Qin, E.B. Wang, Y.G. Li, Z.M. Su, L. Xu, L. Carlucci. *Angew. Chem. Int. Ed.*, **44**, 5824 (2005).
[18] X.L. Chen, B. Zhang, H.M. Hu, F. Fu, X.L. Wu, T. Qin, M.L. Yang, G.L. Xue, J.W. Wang. *Cryst. Growth Des.*, **10**, 3706 (2008).
[19] X.Y. Yi, Z.G. Gu, M.F. Wang, H.Y. Jia, H.M. Peng, Y. Ying, X. Gong, W.S. Li, Y.P. Cai. *Inorg. Chem. Commun.*, **14**, 458 (2011).
[20] D.R. Xiao, E.B. Wang, H.Y. An, Y.G. Li, L. Xu. *Cryst. Growth Des.*, **7**, 506 (2007).
[21] S.L. Li, Y.Q. Lan, J.C. Ma, J.F. Ma, Z.M. Su. *Cryst. Growth Des.*, **10**, 1161 (2010).
[22] Z. Su, J. Fan, M. Chen, T. Okamura, W.Y. Sun. *Cryst. Growth Des.*, **11**, 1159 (2011).
[23] G.Z. Liu, S.H. Li, L.Y. Wang. *CrystEngComm.*, **14**, 880 (2012).
[24] P. Lightfoot, A. Snedden. *J. Chem. Soc., Dalton Trans.*, 3549 (1999).
[25] S.W. Lee, H.J. Kim, Y.K. Lee, K. Park, J. Son, Y. Kwon. *Inorg. Chim. Acta*, **353**, 151 (2003).
[26] C.Y. Sun, L.C. Li, L.P. Jin. *Polyhedron*, **25**, 3017 (2006).
[27] M.A. Braverman, R.M. Supkowski, R.L. LaDuca. *Inorg. Chim. Acta*, **360**, 2353 (2007).
[28] J. Tao, M. Tong, X. Chen. *J. Chem. Soc., Dalton Trans.*, 3669 (2000).
[29] X.N. Cheng, W.X. Zhang, Y.Y. Lin, Y.Z. Zheng, X.M. Chen. *Adv. Mater.*, **19**, 1494 (2007).
[30] J.J. Wang, L.J. Gao, P.X. Cao, Y.P. Wu, F. Fu, M.L. Zhang, Y.X. Ren, X.Y. Hou. *J. Coord. Chem.*, **65**, 3614 (2012).
[31] Y.N. Zhang, X. Hai, Y.T. Li, L. Cui, Y.Y. Wang. *J. Coord. Chem.*, **65**, 2724 (2012).
[32] J. Qu, Y.L. Yi, Y.M. Hu, W.T. Chen, H.L. Gao, J.Z. Cui, B. Zhai. *J. Coord. Chem.*, **65**, 3740 (2012).
[33] G.M. Sheldrick. *SHELXS-97 and SHELXL-97, Program for X-ray Crystal Structure Solution and Refinement*, Göttingen University, Germany (1997).
[34] O.K. Kwak, K.S. Min, B.G. Kim. *Inorg. Chim. Acta*, **360**, 1678 (2007).
[35] H.C. Garcia, R.T. Cunha, R. Diniz, L.F.C. de Oliveira. *J. Mol. Struct.*, **991**, 136 (2011).
[36] J.Y. Sun, H.Z. Xu. *Inorg. Chem. Commun.*, **14**, 254 (2011).
[37] S. Zhang, Z. Wang, H.H. Zhang, Y.N. Cao, Y.X. Sun, Y.P. Chen, C.C. Huang, X.H. Yu. *Inorg. Chim. Acta*, **360**, 2704 (2007).
[38] X.L. Chen, T. Qin, H.M. Hu, F. Fu, B. Zhang, X.L. Wu, M.L. Yang, G.L. Xue, L.F. Xu. *Inorg. Chem. Commun.*, **11**, 28 (2008).
[39] J.W. Ye, P. Zhang, K.Q. Ye, H.Y. Zhang, S.M. Jiang, L. Ye, G.D. Yang, Y. Wang. *J. Solid State Chem.*, **179**, 438 (2006).
[40] B. Valeur. *Molecular Fluorescence: Principles and Applications*, Wiley-VCH, Weinheim (2002).
[41] S.L. Zheng, J.H. Yang, X.L. Yu, X.M. Chen, W.T. Wong. *Inorg. Chem.*, **43**, 830 (2004).
[42] L.Y. Zhang, G.F. Liu, S.L. Zheng, B.H. Ye, X.M. Zhang, X.M. Chen. *Eur. J. Inorg. Chem.*, **16**, 2965 (2003).
[43] X.Z. Sun, Z.L. Huang, H.Z. Wang, B.H. Ye, X.M. Chen. *Z. Anorg. Allg. Chem.*, **631**, 919 (2005).